J. Appl. Cryst. (1986). **19**, 267–272

Correction of Intensities for Preferred Orientation in Powder Diffractometry: Application of the March Model

BY W. A. DOLLASE

Department of Earth and Space Sciences, University of California at Los Angeles, Los Angeles, CA 90024, USA

(*Received 24 September 1985; accepted 3 April 1986*)

Abstract

Diffracted intensities from axially symmetric flat-plate or capillary specimens, composed of effectively rod- or disk-shaped crystallites, can be corrected for preferred orientation with a single pole-density profile. A convenient procedure is to approximate this profile with a function whose variable parameters are fit during least-squares structure refinement. Several functions have previously been suggested but without theoretical justification. The present study reviews the derivation of this method and examines its assumptions and applications. The several proposed functions are compared with each other and with the March function which describes the pole-density distribution produced by rigid-body rotation of inequant crystallites (*i.e.* crystallites with unequal sides) upon axially symmetric volume-conserving compression or expansion. For its basis, ease of use, single variable parameter, direct interpretability and good refinement test results, the March distribution is proposed as an advantageous pole-density profile function for general use.

Introduction

It has become routine practice to include, in the least-squares refinement step of crystal-structure refinement, a scheme which corrects powder intensity data for the effects of preferred orientation (Rietveld, 1969; Young & Wiles, 1981; Will, Parrish & Huang, 1983). This paper examines the assumptions and methods used in such correction schemes and introduces an alternative function, based on that of March (1932), which has some advantages.

Geometry of preferred orientation

The geometries of the two most common sample configurations are shown in Fig. 1. In these projections onto the unit sphere, *I*, *D* and *O* define, respectively, the incident and diffracted beam and their bisector, the scattering vector. In flat-plate geometry the sample normal is parallel to the scattering vector. The dotted lines in the figure represent contours of equal density of poles to some specific plane. The total intensity diffracted by a plane will be proportional to the density of poles to this plane at the location corresponding to the scattering vector, *i.e.*

$$I_h = sLP_h(O)F_h^2, \qquad (1)$$

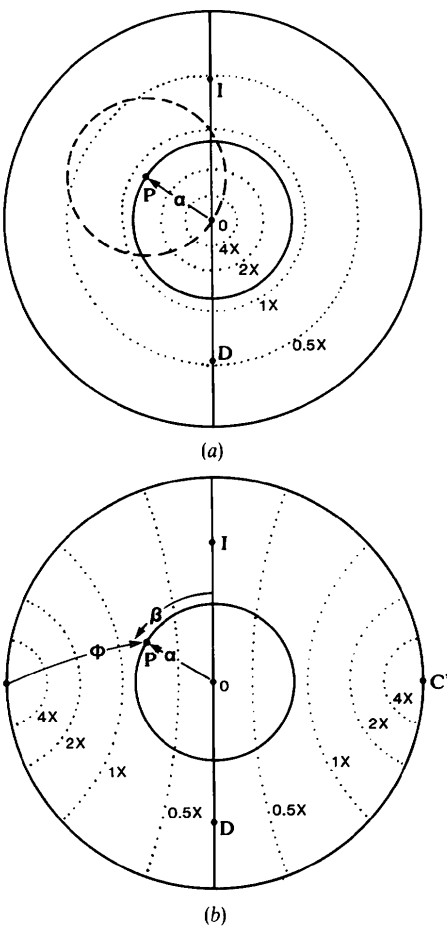

Fig. 1. (*a*) Contour plot of pole density of the preferred-orientation plane for a flat-plate specimen projected onto the unit sphere. *I*, *D* and *O* refer to the directions of the incident and diffracted beams and the scattering vector, respectively. (*b*) Contour plot of pole density of the preferred-orientation plane for a hypothetical filled-capillary specimen. The capillary axis is *CC'*.

0021-8898/86/040267-06$01.50

where s is the scale factor, L is the combined Lorentz, polarization and monochromator factors, $P_h(O)$ is the density of (hkl) poles at the scattering vector, and F_h is the structure factor for reflection hkl.

In theory, $P_h(O)$, as well as the pole density at any other location, could be determined from complete analysis of specimen texture by measuring pole-density distributions of a number of diffracting planes followed by inversion of the data to yield pole densities for all other, unmeasured, planes (see, for example, Roe & Krigbaum, 1964; Bunge, 1985). Such measurements require a (multiaxis) pole-figure goniometer and correction for such effects as absorption, defocusing and surface roughness. A variant of this approach, termed the 'symmetrized harmonic' method, involves representing the pole figures by a sum of spherical harmonic terms and has been applied by Järvinen, Merisalo, Pesonen & Inkinen (1970), Pesonen, Järvinen & Kurki-Suonio (1973) and Pesonen (1979) to specimens of cubic, hexagonal and tetragonal crystallites, respectively. The specimen is required to show cylindrical symmetry and the number of pole figures which must be measured, as well as the number of harmonics required to approximate the pole densities, depends on the degree of preferred orientation.

A more widely used alternative correction method exists which does not require a multiaxis diffractometer and can be applied to crystals of any symmetry. This method assumes that the sample has cylindrical (axial) symmetry and that the sample crystallites are effectively rod or disk shaped. The first assumption usually follows from common methods of sample preparation and can be ensured by spinning the sample about its cylindrical axis during data measurement. The second assumption requires further examination.

The disk- or rod-shaped crystallite model

Preferred orientation usually results from processes such as compaction, settling or deformation acting on non-isotropic crystallite shapes. To a first approximation, inequant grains can be described as either platy (having one shorter dimension) or elongated (having one longer dimension). The prominent planar surface of platy crystallites (often a cleavage or growth face) will be referred to as the preferred orientation plane and designated (HKL). For rod-shaped crystallites (HKL) is the (rational or irrational) plane normal to the prominent elongation axis. Crystallite cross sections parallel to (HKL) are often approximately circular when averaged over all crystallites in the sample. Crystallites whose average shape conforms to this description are effectively disk or rod shaped.

Settling and compaction of platy crystallites in a flat-plate sample result in a distribution of poles to (HKL) of the type shown in Fig. 1(*a*). For a diffraction plane, (hkl), which makes an angle α with (HKL) to contribute to the diffracted intensity a crystallite must have the pole to (HKL) somewhere on a circle of radius α centered on the sample normal (the unbroken inner circle in Fig. 1). Let P be the pole to one of these candidate diffracting crystallites. With the pole to (HKL) at P, the pole to (hkl) must lie somewhere on the dashed circle of radius α centered on P. The second assumption of the rod or disk model is that there is an equal probability of finding the pole to (hkl) at any point on this dashed circle. If this crystallite were rotated about its (HKL) pole, the pole to (hkl) would migrate around the dashed circle. If the crystallites are effectively disk or rod shaped any of these rotational orientations is equally likely, at least on a statistical basis, and the second assumption is satisfied.

Given a uniform likelihood of finding the (hkl) pole at any azimuth around the pole to (HKL), the density of (hkl) poles at the sample normal is equal to the density of (HKL) poles at an angle α from the sample normal. That is,

$$P_h(O) = P_H(\alpha), \tag{2}$$

where α is the angle between (hkl) and (HKL). Thus for the flat-plate sample, the problem of determining the preferred orientation correction factor, $P_h(O)$, for each reflection reduces to finding the one-dimensional pole-density profile, $P_H(\alpha)$, of the preferred orientation plane.

In the case of a capillary sample the distribution of (HKL) poles is axially symmetric about the capillary axis and can be described by a one-dimensional pole-density distribution, $P_H(\varphi)$, an example of which is shown in Fig. 1(*b*). The set of preferred orientation correction factors which constitute the one-dimensional profile, $\hat{P}_H(\alpha)$, may be obtained from $P_H(\varphi)$. The derivation of $\hat{P}_H(\alpha)$ is the same as the derivation of $P_H(\alpha)$ except for one step. For a capillary, the density of (HKL) poles at an angle α from the scattering vector is no longer constant but varies as a function of the pole-density coordinates α and β (Fig. 1*b*). Consequently, $P_h(O)$ is equal to the average (HKL) pole density at an angle α from the scattering vector, that is, the average value found along the unbroken inner circle shown in Fig. 1(*b*). This average may be obtained by integration:

$$P_h(O) = \hat{P}_H(\alpha) = 2/\pi \int_0^{\pi/2} P_H(\alpha, \beta)\mathrm{d}\beta. \tag{3}$$

If the axial pole-density profile, $P_H(\varphi)$, is known, $\hat{P}_H(\alpha)$ may be obtained by numerical integration making use of the relation among coordinates: $\varphi = \cos^{-1}(\sin\alpha \sin\beta)$.

Table 1. *Mathematical forms of proposed pole-figure profiles*

α is the angle from the scattering vector and G, b and r are adjustable coefficients which reflect the strength of the preferred orientation.

No.	Max. at $\alpha = 0$	Min. at $\alpha = 0$	Reference
1	$\exp[-G\alpha^2]$	$\exp[-G(\pi/2-\alpha)^2]$	(1), (2)
2	$\exp[G(\pi/2-\alpha)^2]$	$\exp[G\alpha^2]$	(3), (4)
3	$\exp[-G\sin^2\alpha]$	$\exp[-G\cos^2\alpha]$	(5)
4	$\exp[-G(1-\cos^3\alpha)]$	$\exp[-G(1-\sin^3\alpha)]$	(5)
5	$b+(1-b)\exp[-G\alpha^2]$	$b+(1-b)\exp[-G(\pi/2-\alpha)^2]$	(6), (7)
6	$(r^2\cos^2\alpha + r^{-1}\sin^2\alpha)^{-3/2}$		(8)

References: (1) Uda (1967); (2) Rietveld (1969); (3) Parrish & Huang (1983); (4) Will, Parrish & Huang (1983); (5) Capkova & Valdova (1974); (6) Sasa & Uda (1976); (7) Toraya & Marumo (1981); (8) March (1932).

Effect of symmetry-equivalent reflections

With powder samples, a peak observed at some particular diffraction angle, 2θ, is generally due to diffraction from several symmetry-equivalent planes. Except in special cases, the various planes of a symmetry-equivalent set do not make the same angle with a specified preferred orientation plane. As a result, the pole densities for each of the contributing planes will, in general, differ and so

$$I_{2\theta} = sL\left[\sum_{i=1}^{m} P_H(\alpha_i)\right]F_h^2 \qquad (4)$$

where α_i refers to the angle between (HKL) and the ith member of the symmetry-equivalent set of m diffracting planes. The preferred orientation plane itself is a member of some set of symmetry-equivalent planes. If the dominant morphological feature of the crystallites is reindexed as some other member of this set, the individual values of α_i in (4) will be permuted but the sum of terms remains the same. This sum can be considered as a generalized multiplicity term.

Pole-density profiles

Several ways have been suggested to determine the $P_H(\alpha)$ profile. One method is to measure it experimentally. Again, this requires a multiaxis goniometer and correction of the measurements for the effects of tilting the sample. Examples of measured pole-figure profiles have been given by de Wolff & Sas (1969) for $Cd(OH)_2$ and by Capkova & Valdova (1974) for variously prepared samples of magnesium.

An increasingly popular method of determining $P_H(\alpha)$ is to assign it some specific functional form having a small number of coefficients which are adjusted during crystal-structure refinement to maximize the fit between observed and calculated intensities. Several different functional forms have been employed to approximate P_H and another will be introduced here. Before discussing them it is useful to consider the general properties of $P_H(\alpha)$ as a probability distribution function. These include the following: the integral of P_H over all orientations is unity, $P_H(\alpha)$ can be expected to be symmetric across $\alpha = 0$ and $\pi/2$ and, considering the processes that produce preferred orientation, it can also be expected that there will be no cusp at $\alpha = 0$ or $\pi/2$, *i.e.* the first derivative with respect to α will be zero at these points. These general expectations seem to be supported by the measured pole-density profiles.

The various profile functions that have been suggested are collected in Table 1. Each of these describes a curve either with its maximum at $\alpha = 0$ falling off smoothly towards a minimum at $\alpha = \pi/2$, or *vice versa.* For each function only the form with its maximum at 0 was reported but the extension to the corresponding alternative form is unambiguous. Which functional form applies (that is, whether the maximum is at 0 or $\pi/2$) depends on crystallite shape (disk or rod approximation), method of sample preparation (effective sample compaction or extension) and sample geometry (flat plate or capillary).

For a very weakly developed preferred orientation any one of these functions (other than no. 5) would probably give as good a correction as any other. (With expression no. 5, as G approaches 0, the value of b becomes indeterminate.) With even a modest degree of preferred orientation, however, the shapes of the different functions begin to diverge significantly. Some of the functions suggested seem to be better suited to real textures than others. None of the previously suggested profile functions conform to all the general properties of a probability distribution. None (other than no. 6) are normalized to unit integral which means that a change in an adjustable coefficient must be counterbalanced by a change in the overall scale factor. Expression no. 2 is a non-Gaussian exponential whose concave shape and nonzero derivatives at $\alpha = 0, \pi/2$ do not match published pole figures. It has been noted that in the Gaussian expression (no. 1), if G is large enough to fit even a moderate maximum in the pole figure, $\exp[-G\alpha^2]$ predicts much too low a pole density at high angles (Sasa & Uda, 1976; Toraya & Marumo, 1981). This, in fact, was the reason for

adding a second adjustable parameter in the form of a constant, giving expression no. 5.

In 1932, March published a study of the development of preferred orientation as a result of rigid-body rotation of platy or rod-shaped grains upon linear sample deformation. The March model has been highly successful in describing, in detail, the textures found in natural and synthetic deformed materials and in quantitatively relating deformation to preferred orientation (Oertel, 1985). For the special case of a cylindrically symmetric specimen produced by a volume-conserving compression or extension along the cylindrical axis, the pole density is given by equation no. 6 in Table 1. The March coefficient, r, characterizes the strength of the preferred orientation (pole density ranges from r^{-3} to $r^{3/2}$) and is related to the amount of sample deformation. With the March function the same formulation is used for a pole-density maximum at $\alpha = 0$ ($r < 1$) or a pole-density maximum at $\alpha = \pi/2$ ($r > 1$). Because the orientations of platy and acicular crystallites are differently defined relative to their respective morphologies, there is a different relationship between the March variable, r, and the sample compaction or extension for the two limiting crystallite shapes. For platy crystallites the relation is $r = d/d_0$, where d_0 is the thickness of an original (hypothetical) sample showing uniform pole density and d is the sample thickness after axial extension or compaction. For acicular crystallites the relation is $r = d_0/d$.

The March distribution has a number of advantages: (1) it has a valid theoretical basis related to the major mechanism (grain rotation) that produces preferred orientation; (2) it is a true probability distribution with unit integral and is symmetric and smooth across $\alpha = 0$ and $\pi/2$; (3) the same expression applies to both grain shapes; (4) it has a single variable parameter. Even when samples develop preferred orientation due to mechanisms other than compaction and grain settling, fitting a March distribution allows estimation of an intuitively simple equivalent specimen compaction which is useful for quantitative comparison of samples. For all these reasons the March distribution is proposed here as an alternative pole-figure profile function of direct applicability in preferred-orientation correction.

Comparative test of profile functions

Calcite

X-ray diffraction data sets were measured on powders of $CaCO_3$ (space group $R\bar{3}c$). The calcite samples were fine-grained Dover chalk and reagent-grade calcium carbonate. The preferred orientation plane, corresponding to the excellent cleavage, is $(10\bar{1}4)$ referred to hexagonal axes. Least-squares structure refinements were made with 35 integrated intensities measured on flat-plate samples. There are four variable parameters with Gaussian or March preferred-orientation corrections or five variables if the Gaussian-plus-constant expression is used. The quality of the refinements was judged by comparing R factors and by comparison of the calculated interatomic distances with single-crystal values reported in the literature (Reeder & Wenk, 1983). Refinement using the two-parameter Gaussian-plus-constant equation (no. 5) diverged, at least for the particular starting parameters chosen. The March distribution (no. 6) produced as low an R factor and as plausible a set of interatomic distances as the Gaussian model. However, the degree of preferred orientation in these two samples was too weak [March $r = 0{\cdot}89(5)$] to demonstrate that either function was clearly superior to the other.

Huntite

Huntite, $CaMg_3(CO_3)_4$ (space group $R32$), is known only to occur as aggregates of micrometer-sized grains which demonstrate a well-developed platy $(10\bar{1}1)$ growth form (again referred to hexagonal axes). One of the samples was prepared by loading a fine powder into the $25 \times 15 \times 1$ mm recessed well of a plastic sample holder, lightly moistening with methanol and smoothing with a spatula. This sample yielded R factors of 7·6, 7·6 and 5·3% using no preferred-orientation correction, a Gaussian pole-density profile and a March profile, respectively (86 observed integrated intensities and 11 variable parameters). The addition of a constant term to the Gaussian profile again caused the refinement to diverge because of correlation between this term and the overall scale factor. From the refined value of the March distribution parameter, $r = 0{\cdot}79(1)$, the degree of preferred orientation is equivalent to about 21% sample compaction. Results and further details of this refinement are given elsewhere (Dollase & Reeder, 1986).

A second huntite sample with stronger preferred orientation was prepared by adding drops of water to a small amount of powdered sample, stirring to form a watery slurry and then allowing the slurry to settle and dry on a flat glass plate. 60 integrated intensities were measured and least-squares refinements of the 10 or 11 variable parameters were made using each of the functions listed in Table 1. Without a preferred-orientation correction an R factor of 29% and unreasonably high temperature factors were obtained. The results obtained with the various profile functions, all of which gave plausible temperature factors, fall into two groups. A simple Gaussian (no. 1) or exponential (no. 2) profile gave R factors of 10% while the remaining pole-figure profiles all gave R factors of 6 to 7%. Fig. 2 compares these best-fit $(10\bar{1}1)$ pole-figure profiles obtained for the slurried huntite specimen. There

are no observed data points shown in Fig. 2 because all observed peaks (other than 000*l* reflections) are the sum of three or six superimposed planes which make different angles with the preferred-orientation plane.

For this highly oriented water-sedimented sample, the effective compaction, estimated from the March distribution parameter of $r = 0{\cdot}57(1)$, corresponds to a 43% flattening of a uniform distribution. The maximum pole densities are about 6X. Fig. 2 illustrates that the Gaussian expression (no. 1) yields a much lower pole density at high angles than do any of the more successful profile functions. On the other hand, the non-Gaussian exponential (no. 2) gives the highest pole density at high angles, but at the expense of a rather implausible shape at low α angles. The remaining profiles have a similar shape, as would be expected from their similar residuals. The reasonable *R* factors obtained on this strongly oriented sample with the use of a March distribution or either of Capkova & Valdova's trigonometric functions support the use of these profile functions in preferred-orientation correction. As the two-parameter Gaussian-plus-constant function did not give a significantly lower residual than several of the one-parameter functions, its use seems unwarranted.

Capillary sample simulations

A number of tests were made by simulating an (*HKL*) pole-density distribution for a capillary sample, $P_H(\varphi)$, which conformed to one of the profile functions of Table 1, and then obtaining the corresponding correction-factor profile, $\hat{P}_H(\alpha)$, from (4). Provided that the degree of preferred orientation in $P_H(\varphi)$ is not too strong, the transformed profile, $\hat{P}_H(\alpha)$, is rather similar to its parent distribution [although the locations of maxima are interchanged and the range between maximum and minimum values is reduced relative to $P_H(\varphi)$]. With textures whose maximum pole densities are 2X, the deviation of $\hat{P}_H(\alpha)$ from the same functional forms as $P_H(\varphi)$ amounts to less than 2% for the trigonometric functions nos. 3, 4 and 6 of Table 1, but is generally greater for the remaining functions. For stronger degrees of preferred orientation, $\hat{P}_H(\alpha)$ may still be closely approximated by one of these profile functions but $P_H(\varphi)$ must then correspond to some other functional form.

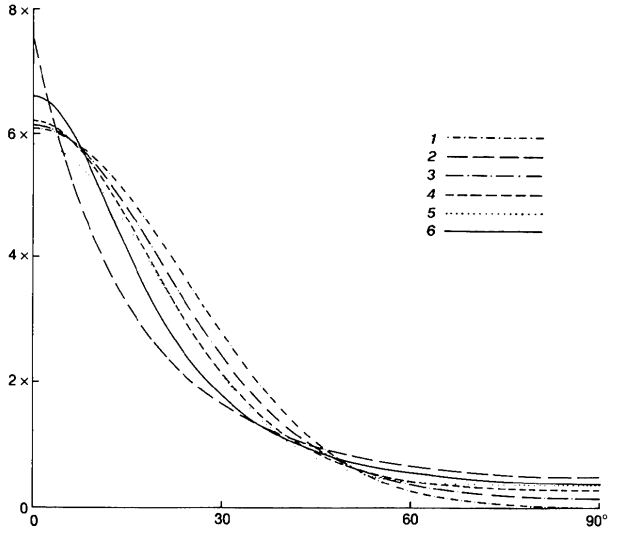

Fig. 2. Fitted (10$\bar{1}$1) pole-figure profiles in slurried huntite specimen. The curve numbers refer to the profile functions listed in Table 1.

Extensions

There is a need for further comparative tests of profile functions. It would also be useful to compare them with directly measured pole-density profiles. In addition, the rod- or disk-shaped model needs to be further refined. One obvious extension is the inclusion of a second, independent, population of crystallites. Thus, a powder could be modeled as a given volume fraction with one preferred-orientation plane and strength of preferred orientation plus the remaining volume fraction with the same or another preferred-orientation plane and strength of preferred orientation. That is, for each reflection *h*,

$$I_h = sL[xP_{H1}(\alpha_1) + (1 - x)P_{H2}(\alpha_2)]F_h^2 \qquad (5)$$

where x and $(1 - x)$ represent the volume fractions of crystallites dominated by preferred-orientation planes (H_1) and (H_2), respectively, Such a treatment would add two more variables per additional population but might be reasonable in cases where there are two (or more) competing preferred-orientation planes or more than one distinct population of crystallites having the same preferred-orientation plane. An example of the former would be a powder of a material showing two crystallographically independent cleavages, and an example of the latter would be a powder consisting of a small proportion of coarser crystallites showing well developed inequant morphology embedded in a matrix of finer crystallites showing only a weak development of the same morphology.

I am indebted to Gerhard Oertel for introducing me to the March model and, along with Charles Ross, for helpful reviews of the manuscript. Charles Prewitt kindly provided use of the powder diffractometer system at SUNY, Stony Brook, and samples were provided by Rich Reeder and Don Lindsley. I also thank an anonymous reviewer for pointing out the Capkova & Valdova (1974) reference.

References

BUNGE, H. J. (1985). In *Preferred Orientation in Deformed Metals and Rocks*, edited by H.-R. WENK, pp. 73–108. Orlando: Academic Press.

CAPKOVA, P. & VALDOVA, V. (1974). *Czech. J. Phys.* **B24**, 891–900.

DOLLASE, W. A. & REEDER, R. J. (1986). *Am. Mineral.* **71**, 163–166.

JÄRVINEN, M., MERISALO, M., PESONEN, A. & INKINEN, O. (1970). *J. Appl. Cryst.* **3**, 313–318.

MARCH, A. (1932). *Z. Kristallogr.* **81**, 285–297.

OERTEL, G. (1985). In *Preferred Orientation in Deformed Metals and Rocks*, edited by H.-R. WENK, pp. 259–265. Orlando: Academic Press.

PARRISH, W. & HUANG, T. C. (1983). *Adv. X-ray Anal.* **26**, 35–44.

PESONEN, A. (1979). *J. Appl. Cryst.* **12**, 460–463.

PESONEN, A., JÄRVINEN, M. & KURKI-SUONIO, K. (1973). *Phys. Fenn.* **8**, 81–91.

REEDER, R. J. & WENK, H.-R. (1983). *Am. Mineral.* **68**, 769–776.

RIETVELD, H. M. (1969). *J. Appl. Cryst.* **2**, 65–71.

ROE, R. J. & KRIGBAUM, W. R. (1964). *J. Chem. Phys.* **40**, 2608–2615.

SASA, Y. & UDA, M. (1976). *J. Solid State Chem.* **18**, 63–68.

TORAYA, H. & MARUMO, F. (1981). *Mineral. J.* **10**, 211–221.

UDA, M. (1967). *Z. Anorg. Allg. Chem.* **350**, 105–109.

WILL, G., PARRISH, W. & HUANG, T. C. (1983). *J. Appl. Cryst.* **16**, 611–622.

WOLFF, P. M. DE & SAS, W. H. (1969). *Acta Cryst.* **A25**, 206–209.

YOUNG, R. A. & WILES, D. B. (1981). *Adv. X-ray Anal.* **24**, 1–23.